Computational Study of Hydrogen Shifts and Ring-Opening Mechanisms in alpha-Pinene Ozonolysis Products

Kurten, Theo

2015-11-19

Kurten , T , Rissanen , M P , Mackeprang , K , Thornton , J A , Hyttinen , N , Jorgensen , S , Ehn , M & Kjaergaard , H G 2015 , ' Computational Study of Hydrogen Shifts and Ring-Opening Mechanisms in alpha-Pinene Ozonolysis Products ' , Journal of Physical Chemistry A , vol. 119 , no. 46 , pp. 11366-11375 . https://doi.org/10.1021/acs.jpca.5b08948

http://hdl.handle.net/10138/318933
https://doi.org/10.1021/acs.jpca.5b08948

acceptedVersion

A Computational Study of Hydrogen Shifts and Ring-Opening Mechanisms in α-pinene Ozonolysis Products

Journal:	*The Journal of Physical Chemistry*
Manuscript ID	jp-2015-08948j.R1
Manuscript Type:	Article
Date Submitted by the Author:	n/a
Complete List of Authors:	Kurtén, Theo; University of Helsinki, Laboratory of Physical Chemistry, Department of Chemistry Rissanen, Matti; University of Helsinki, Physics Mackeprang, Kasper; University of Copenhagen, Chemistry Thornton, Joel; University of Washington, Seattle, Atmospheric Sciences Hyttinen, Noora; University of Helsinki, Chemistry Jørgensen, Solvejg; University of Copenhagen, Chemistry Ehn, Mikael; University of Helsinki, Department of Physical Sciences, Kjaergaard, Henrik; Copenhagen University, Chemistry

A Computational Study of Hydrogen Shifts and Ring-Opening Mechanisms in α-pinene Ozonolysis Products

Theo Kurtén[1], Matti P. Rissanen[2], Kasper Mackeprang[3], Joel A. Thornton[4], Noora Hyttinen[1], Solvejg Jørgensen[3], Mikael Ehn[2] and Henrik G. Kjaergaard[3]*

[1] Department of Chemistry, University of Helsinki, P.O. Box 55, 00014 Helsinki, Finland

[2]Department of Physics, University of Helsinki, P.O. Box 64, 00014 Helsinki, Finland

[3] Department of Chemistry, University of Copenhagen, Universitetsparken 5, 2100 Copenhagen Ø, Denmark

[4] Department of Atmospheric Sciences, University of Washington, Seattle, Washington 98195, United States

KEYWORDS Atmospheric oxidation, autoxidation, α-pinene, peroxy radicals, hydrogen shifts, secondary organic aerosol

ABSTRACT Autoxidation by sequential peroxy radical hydrogen shifts (H-shifts) and O_2 additions has recently emerged as a promising mechanism for the rapid formation of highly oxidized, low-volatility organic compounds in the atmosphere. A key prerequisite for

autoxidation is that the H-shifts of the initial peroxy radicals formed by e.g. OH or O_3 oxidation are fast enough to compete with bimolecular sink reactions. In most atmospheric conditions, these restrict the lifetime of peroxy radicals to be on the order of seconds. We have systematically investigated all potentially important (non-methyl, sterically unhindered) H-shifts of all four peroxy radicals formed in the ozonolysis of α-pinene using density functional (ωB97XD) and coupled cluster [CCSD(T)-F12] theory. In contrast to the related but chemically simpler cyclohexene ozonolysis system, none of the calculated H-shifts have rate constants above 1 s^{-1} at 298 K, and most are below 0.01 s^{-1}. The low rate constants are connected to the presence of the strained cyclobutyl ring in the α-pinene-derived peroxy radicals, which hinders H-shifts both from and across the ring. For autoxidation to yield the experimentally observed highly oxidized products in the α-pinene ozonolysis system, additional ring-opening reaction mechanisms breaking the cyclobutyl ring are therefore needed. We further investigate possible uni- and bimolecular pathways for opening the cyclobutyl ring in the α-pinene ozonolysis system.

Introduction

Atmospheric aerosol particles play a key role in regulating the Earth's climate, and are responsible for most air pollution-related mortality.[1] A large fraction of these particles consist of secondary organic aerosol (SOA) material, formed from gas-phase precursors (often denoted as volatile organic compounds; VOC) by oxidation reactions.[2]

Since the addition of molecular oxygen (O_2) to most stable molecules is spin-forbidden and thus extremely slow, the oxidation pathways in the troposphere must be initiated by a small number of photochemically generated oxidants, such as OH, O_3, Cl and NO_3.[3] Oxidants

generally react with VOC molecules to form alkyl radicals, to which O_2 can then rapidly add with a pseudo-unimolecular rate constant on the order of 10^7 s^{-1} in atmospheric conditions. The immediate product of this addition reaction is a peroxy radical, commonly referred to as RO_2. Peroxy radicals are thus crucial intermediates in almost any atmospheric oxidation processes,[4,5] and especially in those leading to the formation of condensable vapors and hence SOA.[6]

Recent experimental and theoretical research on atmospheric oxidation further emphasizes the importance of peroxy radical chemistry in SOA formation. According to these studies, autoxidation - a chain of unimolecular peroxy radical hydrogen shifts (H-shifts) and O_2 additions, followed by uni- or bimolecular termination reactions - can lead to the rapid formation of closed-shell products with O:C ratios around or above one. Due to their high O:C ratio and multitude of hydrogen-bonding functional groups, these products have been denoted "ELVOC", Extremely Low Volatility Organic Compounds.[7] Autoxidation by H-shifts is well known in other chemical systems such as low-temperature combustion[8], and H-shifts in peroxy radicals have been theoretically proposed to take place in the atmospheric oxidation of both isoprene[9] and α-pinene.[10] The laboratory oxidation study of pentanone by Crounse et al.[11] was among the first direct experimental indications that autoxidation may play an important role in atmospheric SOA formation. Subsequently, the mass spectrometric studies by Ehn et al.[12], Rissanen et al.[13], Mentel et al[14] and Jokinen et al[15] demonstrated the extreme extent to which autoxidation can proceed under atmospheric conditions.

The mechanism for ELVOC formation via autoxidation has been studied in detail at the molecular level for cyclohexene, using quantum chemical calculations.[13,16] In a follow-up study by Rissanen et al.,[17] the same mechanism was tentatively shown to apply also for methylcyclohexene ozonolysis, as rapid H-shifts by the first-generation peroxy radicals initiating

the process could be identified. In the same study, autoxidation of the peroxy radicals derived from the ozonolysis of α-pinene was found to be more complicated, as no rapid first-generation H-shifts could be identified based on density functional theory (DFT) - level energy barriers. The VOC α-pinene is one of the main monoterpenes emitted by vegetation. It is structurally related to methylcyclohexene, but contains two additional methyl groups and a cyclobutyl ring (see Figure 1 for illustration and carbon numbering scheme). In contrast to the cyclohexenes, the α-pinene molecule thus contains two ring structures, of which one breaks during the ozonolysis reaction, as the double bond between carbon atoms 2 and 3 is broken. Carbon atoms 2 and 4 in the ozonolysis products remain arranged in a "*cis*" pattern on the same side of the surviving cyclobutyl ring, rather than in a "*trans*" pattern. The latter is energetically more favorable once the C=C bond is broken, but impossible to reach without breaking multiple C-C bonds. Unfortunately, the configurational sampling algorithm applied in Rissanen et al.[17] led to the *trans* structural isomers being used for the two computationally studied peroxy radicals originating from α-pinene ozonolysis.

In this study, we systematically investigate all potentially important H-shifts for all four peroxy radicals originating from α-pinene ozonolysis, using density functional theory with coupled cluster energy corrections. We also investigate possible mechanisms for opening the cyclobutyl ring left intact by ozonolysis, as this would allow additional and probably more rapid H-shift pathways. While the qualitative conclusions on H-shifts in the α-pinene ozonolysis drawn by Rissanen et al.[17] are still valid, the structures and barrier heights computed in the present study should be considered more accurate.

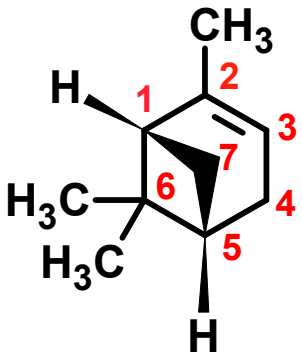

Figure 1. Structure of the α-pinene molecule, with non-methyl carbons numbered. The hydrogen atoms bonded to carbon atoms 1 and 5 are explicitly shown. They are constrained to a *cis* position with respect to each other by the 4-membered ring (as are carbon atoms 2 and 4). They remain *cis* even after the 6-membered ring is broken in the ozonolysis reaction.

Computational details

Initial configurational sampling was carried out using the approach described and validated in Rissanen et al.[13] Briefly, all possible conformers were first generated using the MMFF force field, followed by B3LYP/6-31+G(d) single-point energy evaluations, and subsequent B3LYP/6-31+G(d) optimizations on structures with B3LYP/6-31+G(d) single-point energies within 5 kcal/mol of the lowest-energy conformer. These were all carried out using the Spartan program.[18] In the conformational sampling stage, transition states were treated using constrained minimizations as described in Rissanen et al.[13] Only the isomers that can actually form in the α-pinene ozonolysis reaction, e.g. with respect to *cis-trans* isomery of carbon atoms 2 and 4, were included in our analysis.

The lowest-energy structure for each reactant, transition state and product was then selected for subsequent higher-level treatment at the ωB97XD/aug-cc-pVTZ level[19] using the Gaussian

09 program suite,[20] with tight optimization criteria, and the ultrafine integration grid. Finally, a single-point energy calculation was performed on the ωB97XD/aug-cc-pVTZ optimized structures at the ROHF-ROCCSD(T)-F12a/VDZ-F12 level[21,22] (denoted "F12") using the Molpro 2012.1 program, with default convergence criteria.[23] As shown in Garden et al.,[24] Rissanen et al.[13] and Hyttinen et al.,[16] the B3LYP/6-31+G(d) optimizations provide an excellent estimate of the energy ordering of the conformers, even though the absolute energies calculated at this level are less accurate. The T1 diagnostics for all peroxy radical systems (reactants, transition states and products) were below 0.023 in the CCSD(T)-F12 calculations.

Transition state theory including quantum mechanical tunneling[25] was used to estimate the forward and reverse rate constants (k) of the H-shift reactions:

$$k = \kappa \frac{k_B T}{h} \frac{Q_{TS}}{Q_R} \exp\left(-\frac{E_{TS}-E_R}{k_B T}\right) \qquad (1),$$

where the energies, E_{TS} and E_R, are the zero-point corrected F12 energies of the transition state and reactant, respectively. The quantities Q_R and Q_{TS}, are the partition functions for the reactant, R, and the transition state, TS, respectively. We have used the rigid rotor and the harmonic oscillator approximations to calculate the partition functions. The constants h, k_B, and T are the Planck constant, the Boltzmann constant, and the temperature, respectively. The temperature is set to 298.15 K. The barrier heights for the forward and reverse H-shift reactions, and the imaginary frequency of the transition state, are included in the calculation of the one-dimensional Eckart tunneling factor, κ.[26]

We expect that eq 1 overestimates the H-shift rate constants due to the presence of multiple higher energy conformers ("local minima"), as well as torsional anharmonicity, both of which tend to increase the partition function of the reactants more than that of the transition states. However, based on extensive test calculations on the cyclohexene + O_3 system,[13] these are likely

to affect the rate by less than a factor of 10, especially as the cyclobutyl ring in the peroxy radicals derived from α-pinene ozonolysis restricts both the number of conformers and the number of internal rotation modes compared to the cyclohexene ozonolysis case. Thus, the present approach, where only the lowest-energy conformer is selected for computationally demanding higher level calculations and internal rotor corrections are ignored, should provide a good order-of-magnitude estimate of the H-shift rate constants for the peroxy radicals formed in α-pinene ozonolysis.

Results and Discussion

H-shift reactions of peroxy radicals formed in α-pinene ozonolysis

The first steps of the ozonolysis of alkenes such as α-pinene have been studied extensively.[27,28] The reaction steps leading from ozone and α-pinene to the four possible first-generation peroxy radicals are shown in Figure 2, with additional details discussed in section S1 of the supplementary information.

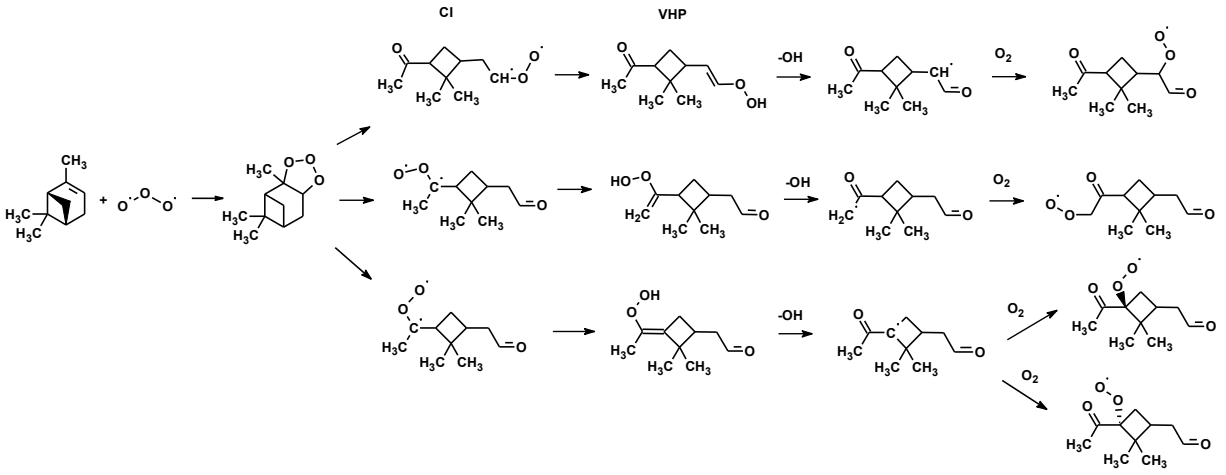

Figure 2. Initial steps of α-pinene ozonolysis. Attack of ozone on the C=C double bond leads to a primary ozonide, which rapidly decomposes, yielding a mixture of four possible Criegee Intermediates (CI), three of which are shown in this figure. 1,4 H-shifts of these three CIs lead to vinylhydroperoxides (VHP), which dissociate to form OH and vinoxy radicals. The vinoxy radicals then add O_2, forming peroxy radicals (RO_2). For the vinoxy radical with the radical center located on the ring, O_2 addition can occur from either direction, giving two different structural isomers as shown in the lower right corner of the figure.

In determining the atmospheric relevance of peroxy radical H-shifts in the α-pinene + O_3 system, the main question concerning the actual ozonolysis mechanism is whether or not all four potentially possible peroxy radical isomers can be expected to form in significant amounts, as predicted e.g. by the MCM model.[29,30] Our calculations verify this to be the case (see section S1 in the Supplementary information for details). The four peroxy radicals formed in the α-pinene + O_3 system have been labeled RO_2a – RO_2d, and are shown in Figure 3.

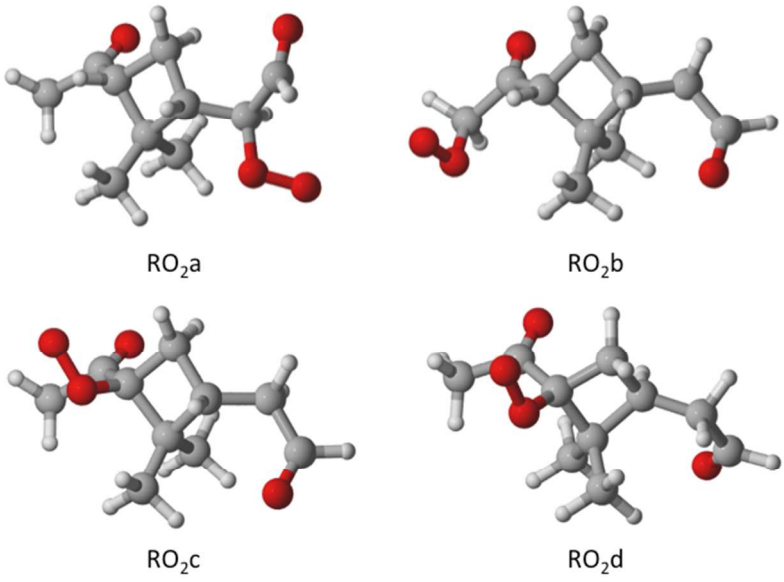

Figure 3: α-pinene ozonolysis yields four different peroxy radicals, labeled RO_2a through RO_2d). Color coding: gray = carbon, red = oxygen, white = hydrogen.

Several structure-activity relationships (SARs) have been proposed for H-abstraction reactions of peroxy radicals,[14,31,32] as well as for the related but more reactive alkoxyradicals.[33] A common feature of these SARs is that abstraction of methyl (-CH_3) hydrogen atoms, as well as abstractions from the carbon atom on which the OO• radical group is located (so-called 1,3 H-shifts in the case of peroxy radicals) are slow compared to other H-shift pathways. Hence, methyl and 1,3 H-shifts were not studied here. In addition, some other H-shifts are made impossible by steric hindrances (e.g. the abstraction of a hydrogen atom where OO and H are on different sides of the four-membered ring). All other H-shift pathways were systematically investigated.

For peroxy radical RO_2a, we considered H-shifts from four different carbon atoms: C1, C3, C5 and C7 (see Figure 4). We were unable to find a transition state for the 1,6 H-shift from C1 due to steric strain, as the hydrogen atom on C5 prevents the OO group from interacting with the hydrogen atom on C1. Of the remaining three H-shifts, the 1,4 H-shift from the aldehydic C3 has the lowest barrier at 20.8 kcal/mol. This is not surprising, as aldehydic H-shifts are known to be fast. For example, the aldehydic 1,4 H-shift in the peroxy radical formed in the OH oxidation of methacrolein was computed by Crounse et al. to have a barrier of 19.0 kcal/mol, using methods very similar to those applied here.[34] Nevertheless, even this barrier is several kcal/mol higher than the most favorable aldehydic H-shifts found in the cyclohexene ozonolysis system.[13] The alternative 1,4 H-shift from C5 has a high barrier of 30.7 kcal/mol. This is explained both by the general relative unfavorability of 1,4 H-shifts, and the difficulty of abstracting hydrogen atoms from small rings, as discussed by Veerecken and Peeters.[35,36] This difficulty is also illustrated by

the relative energy of the C5-centered alkyl radical: while the aldehydic 1,4 H-shift is almost thermoneutral, the 1,4 H-shift from C5 is endothermal by almost 17 kcal/mol. The remaining pathway, a 1,5 H-shift from C7, has a lower barrier and is less endothermal than the H-shift from C5 due to lesser ring strain in both the transition state and the product radical. However, at 25.3 kcal/mol the barrier is still too high to compete with the aldehydic 1,4 H-shift.

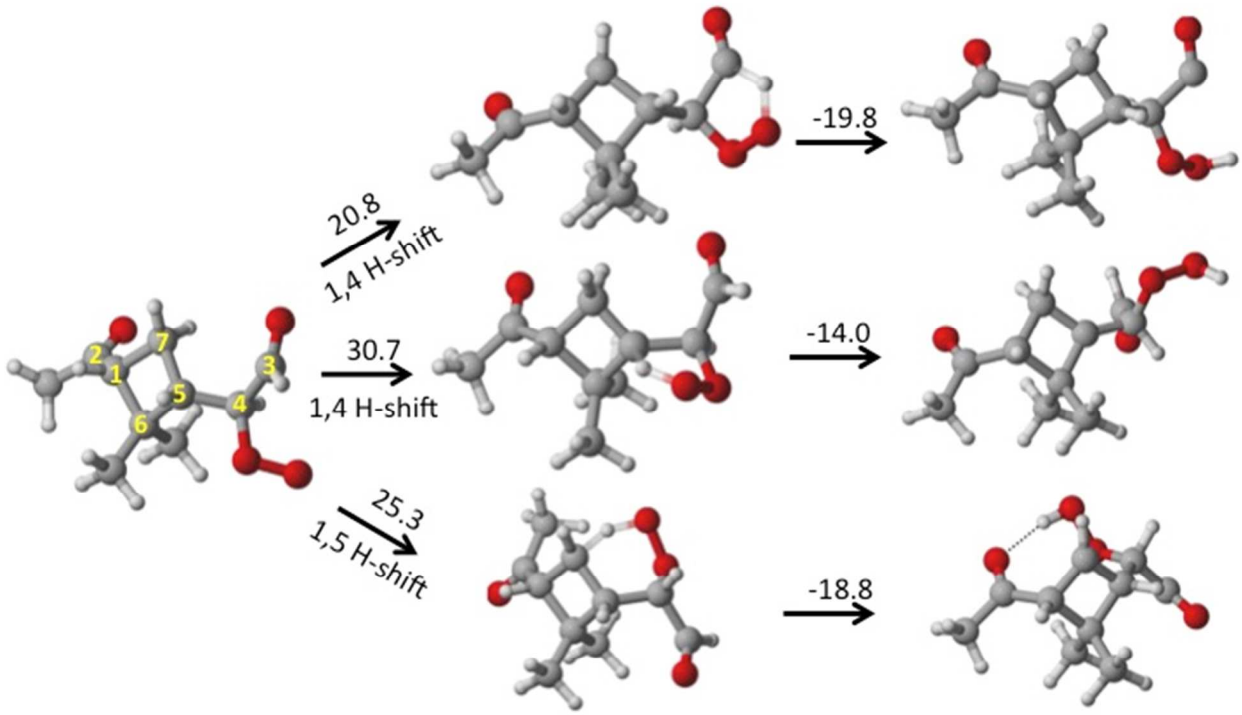

Figure 4: H-shift transition states (middle column) and products (right column) from RO_2a (left). Zero-point corrected F12 relative energies in kcal/mol are given for each step. Color coding as in Figure 3. The non-methyl carbons in the reactant are numbered as in Figure 1.

For peroxy radical RO_2b, we considered H-shifts from five different carbon atoms: C1, C3, C4, C5, and C7 (see Figure 5). We were unable to find transition states for 1,7 and 1,8 H-shifts from C5 and C4, respectively, because the hydrogen atom on C1 prevented the OO group and the respective hydrogen atoms from interacting. This is analogous to the absence of an 1,6 H-shift

from C1 in RO_2a. The most favorable pathway for RO_2b is the 1,5 H-shift from C1. This reaction has a barrier of 22.2 kcal/mol – significantly lower than the corresponding 1,4 H-shift barrier for RO_2a. The aldehydic 1,9 H-shift from C3 has a similar barrier; 22.8 kcal/mol. Presumably, the generally favorable aldehydic H-shift is somewhat sterically hindered by the cyclobutyl ring, and by the need to form a 10-membered ring in the 1,9 H-shift transition state.[11] Somewhat surprisingly, the 1,6 H-shift from C7 has a high barrier at 28.3 kcal/mol. This is 3 kcal/mol higher than the corresponding 1,5 H-shift in RO_2a, possibly due to the additional strain associated with including a carbonyl group (on C2) in the cyclic transition state.[11]

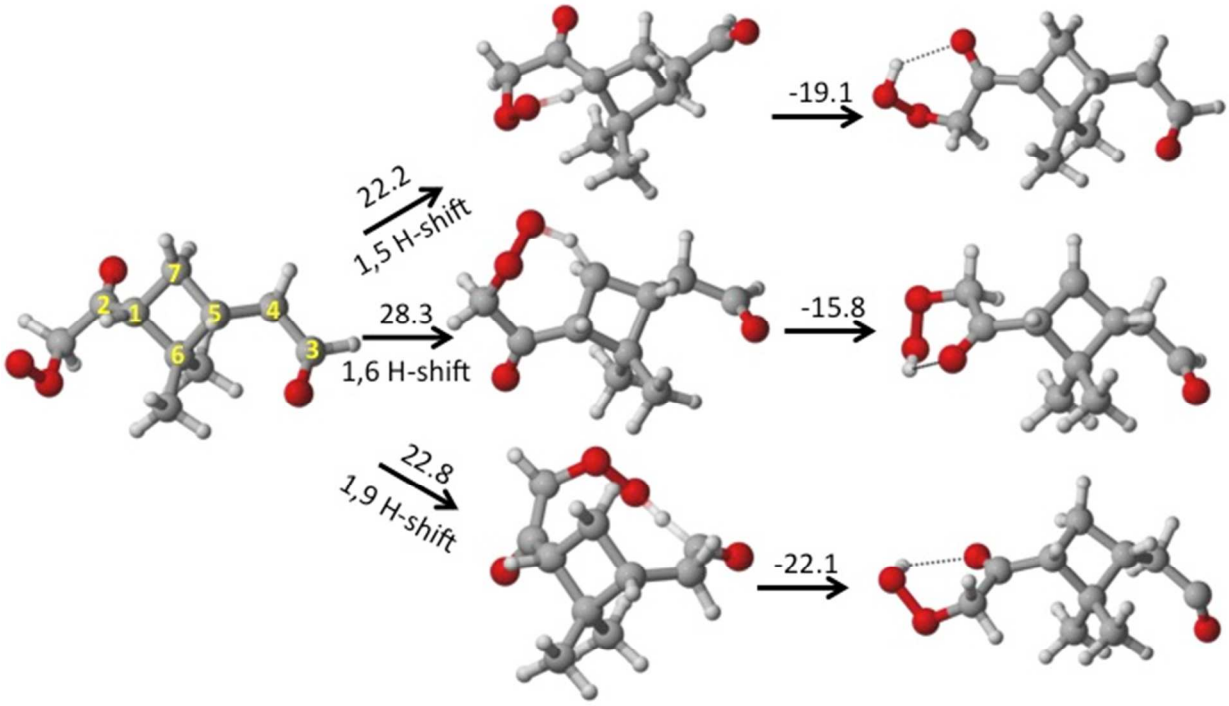

Figure 5: H-shift transition states (middle column) and products (right column) from RO_2b (left). Zero-point corrected F12 relative energies in kcal/mol are given for each step. Color coding as in Figure 3. The non-methyl carbons in the reactant are numbered as in Figure 1.

For peroxy radical RO_2c, we considered H-shifts from four different carbon atoms: C3, C4, C5 and C7 (see Figure 6). Analogously to RO_2a and RO_2b, the C5 hydrogen atom prevents a H-shift from C4. All three possible H-shifts for RO_2c have high barriers. The 1,4 and 1,5 H-shifts from C7 and C5 have barriers of 34.7 and 31.6 kcal/mol, respectively, due to the difficulty of abstracting H-atoms from small rings. Despite aldehydic H-shifts generally being favorable, the 1,7 H-shift from C3 has an extremely high barrier of 63.1 kcal/mol. This is due to the very unfavorable geometry of the transition state, with the RO_2 and the C4-C3 groups being attached in a *trans* configuration, on opposite sides of the cyclobutyl ring.

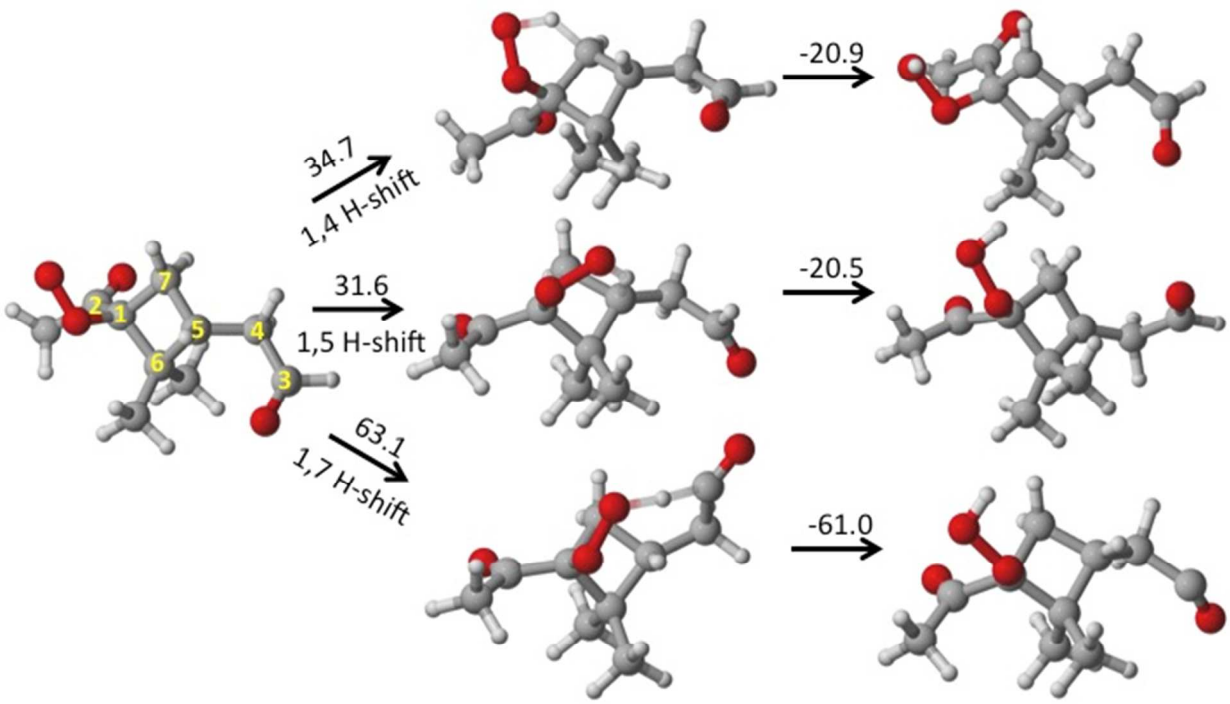

Figure 6: H-shift transition states (middle column) and products (right column) from RO_2c (left). Zero-point corrected F12 relative energies in kcal/mol are given for each step. Color coding as in Figure 3. The non-methyl carbons in the reactant are numbered as in Figure 1.

For peroxy radical RO_2d, we considered H-shifts from three different carbon atoms: C3, C4 and C7 (see Figure 7). In contrast to RO_2c, in RO_2d the hydrogen atom on C5 is on the opposite side of the cyclobutyl ring from the RO_2 group and thus inaccessible for H-shifts. The most competitive pathway is the aldehydic 1,7 H-shift from C3, which has a barrier of 21.2 kcal/mol. This is over 40 kcal/mol lower than the corresponding H-shift of RO_2c, as the reacting groups are now in a *cis* configuration on the same side of the cyclobutyl ring. The 1,6 H-shift from C4 has a moderately high barrier of 27.9 kcal/mol, presumably due to the relative unreactivity of CH_2 hydrogen atoms. The 1,4 H-abstraction from C7 has a high barrier of 35.6 kcal/mol, almost identical to the corresponding reaction of RO_2c.

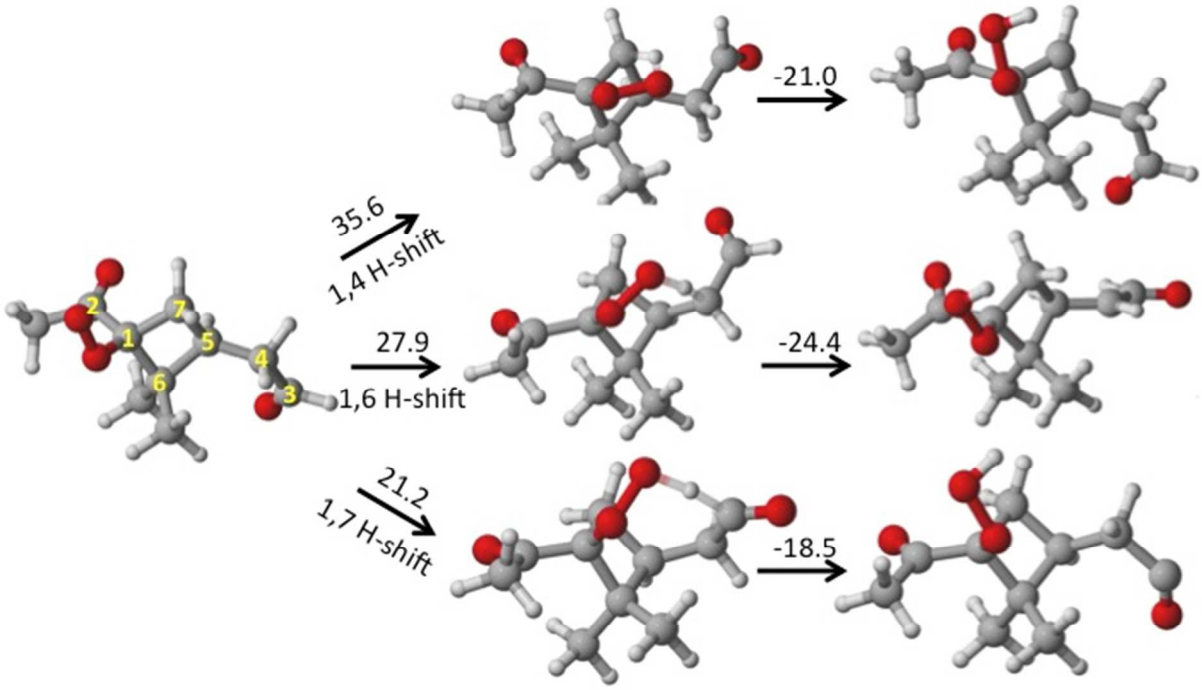

Figure 7: H-shift transition states (middle column) and products (right column) from RO_2d (left). Zero-point corrected F12 relative energies in kcal/mol are given for each step. Color coding as in Figure 3. The non-methyl carbons in the reactant are numbered as in Figure 1.

The barriers and forward rate constants (including tunneling corrections) for all twelve identified H-shifts are shown in Table 1. Tunneling corrections, wavenumbers of the imaginary vibrational modes of the transition states, reverse barriers and reverse rate constants are given in the Supplementary information (section S4).

The rate constants of the H-shifts agree relatively well with previous calculations on similar systems, and structure-activity relationships for peroxy and alkoxy radicals.[11,14,31,32,33,34] All else being equal, aldehydic H-shifts are faster than H-shifts from other sites, and 1,n H-shifts are generally the fastest when n = 5, 6 or 7. Abstractions from hydrogen atoms on the cyclobutyl ring, as well as abstractions across the ring, are slow due to ring strain in the transition state, and (for abstractions from the ring) the energetic penalty of forming alkyl radicals on strained rings.

Reactant	H-shift type	Site type and carbon number	Barrier (kcal/mol)	Rate constant, (s^{-1})
RO_2a	1,4	Aldehydic C3	20.8	0.29
RO_2a	1,4	CH ring C5	30.7	3.1×10^{-7}
RO_2a	1,5	CH_2 ring C7	25.3	4.2×10^{-5}
RO_2b	1,5	CH ring C1	22.2	2.1×10^{-2}
RO_2b	1,6	CH_2 ring C7	28.3	3.9×10^{-7}
RO_2b	1,9	Aldehydic C3	22.8	1.5×10^{-3}
RO_2c	1,4	CH_2 ring C7	34.7	9.3×10^{-9}
RO_2c	1,5	CH ring C5	31.6	7.7×10^{-8}
RO_2c	1,7	Aldehydic C3	63.1	5.7×10^{-26}
RO_2d	1,4	CH_2 ring C7	35.6	1.6×10^{-9}
RO_2d	1,6	CH_2 chain C4	27.9	2.3×10^{-4}
RO_2d	1,7	Aldehydic C3	21.2	0.14

Table 1. Transition state theory rate constants at 298.15 K, including Eckart tunneling corrections, for all H-shift reactions identified in this study. Barriers correspond to zero-point corrected F12 energies.

Despite sizeable tunneling contributions (ranging from 10^2 to 5×10^4, if the anomalous H-shift of RO_2c with a 63.1 kcal/mol barrier is excluded), none of the H-shift rate constants exceeds 1 s^{-1}. We expect that the inclusion of multiconformer and torsional anharmonic effects would tend to decrease rate constants, as the reactants generally have more conformers, and more internal rotors, than the transition states. On the other hand, in applying equation 1 we have neglected the possible excess energy ("chemical activation") of the RO_2 radicals, which would increase the effective reaction rate. We have qualitatively assessed the effect of chemical activation on the two fastest H-shifts of RO_2a by treating its formation from the vinoxy radical and O_2 as a barrierless reaction, which is exothermal by 21.3 kcal/mol (zero-point corrected F12 level). Using the MESMER program (see section S2 of the Supplementary information for details),[37] we found that the excess energy of the formed RO_2a had little effect on the effective rate constant of the H-shifts 298.15 K and 1 atm. The increase is small due to the large number of vibrational degrees of freedom in the system (81 in total), which allows the excess energy to be effectively accommodated. This increases the lifetime of the chemically activated peroxy radical long enough for it to be collisionally stabilized at atmospheric pressure. (This is not surprising: a large fraction of the α-pinene derived Criegee intermediates are also believed to be collisionally stabilized, despite having a slightly lower H-shift barrier and significantly more excess energy.) In low-pressure conditions, the effect of chemical activation will be much larger.

At p=0, chemical activation increases the effective peroxy radical H-shift rates by 3 orders of magnitude or more.

Thus, while the aldehydic H-shifts of RO_2a and RO_2d might just be fast enough for a non-negligible fraction of these radicals to react within a few seconds (the timescale of the flow-tube experiments of Ehn et al.[12] and Rissanen et al.[17]), all the other H-shifts are far too slow. Furthermore, the high H-shift barriers computed here strongly indicate that even if a single of these aldehydic H-shift were to occur, subsequent abstraction sites for the second-generation RO_2 (e.g. all three sites on the cyclobutyl ring) are quite unfavorable, leading to slow second-generation H-shifts, and thereby preventing autoxidation and ELVOC formation.

Possible mechanisms allowing "ELVOC" formation

As shown in the previous section, the H-shifts of the RO_2 species known to be formed in α-pinene ozonolysis are likely too slow to initiate autoxidation on the timescale of flow-tube experiments, or in the atmosphere (due to competing sink reactions). As already tentatively concluded by Rissanen et al,[17] the formation of "ELVOC" molecules with high O:C ratios from the α-pinene + O_3 system therefore almost certainly needs additional reactions beyond the pseudo-unimolecular scheme of H-shifts and O_2 additions proposed for cyclohexene and the methylcyclohexenes.

The main reason for the low rate coefficients of the H-shifts in RO_2a-RO_2d is the presence of the cyclobutyl ring. Therefore, one possible pathway for autoxidation (and thus ELVOC formation) would be a ring-opening reaction in the early part of the oxidation sequence. The ozonolysis reaction itself breaks the cyclohexenyl ring in α-pinene, but leaves the cyclobutyl ring

(comprising carbon atoms 1, 5, 6 and 7 in Figure 1) intact. If also the cyclobutyl ring in the ozonolysis products could be broken, this would increase the number of potentially favorable H-shift sites, as increased ring strain in the product alkyl radicals (and the corresponding H-shift transition states) would no longer be an issue. Based on the H-shift rate constants given in Table 1, breaking of both rings is necessary to obtain the "ELVOC" products with the very high O:C ratios observed in the experiments.

We therefore investigated possible mechanisms for breaking the cyclobutyl ring in the α-pinene ozonolysis products. Based on mechanisms proposed previously for analogous chemical systems, ring-opening can in principle occur at least from three different intermediate products of α-pinene ozonolysis: Criegee intermediates, vinoxy radicals and alkoxy radicals. The three ring-opening mechanisms are shown schematically in Figure 8, and discussed in detail in the following sections.

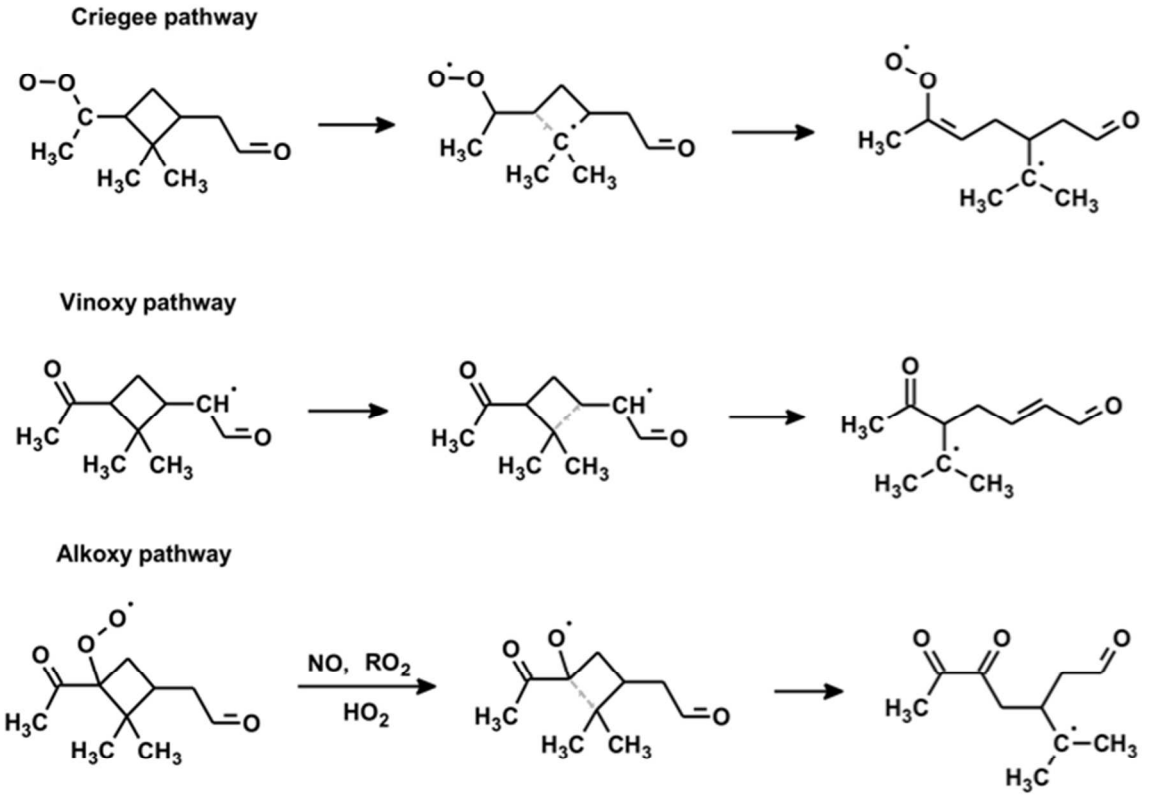

Figure 8. Three possible ring-breaking mechanisms suggested in the literature, as applied to the cyclobutyl ring in the α-pinene + O_3 system.

Ring-opening from Criegee Intermediates

Based on computational results, Nguyen et al.[38] have proposed a pathway for the prompt opening of the cyclobutyl ring in the Criegee intermediates formed in β-pinene ozonolysis. In this reaction, a C-C bond on a carbon atom adjacent to the COO group breaks, leading to a singlet peroxy-alkyl biradical with a new C=C bond. We have found a similar transition state for both Criegee intermediate isomers from α-pinene ozonolysis with the carbonyl oxide group located on the C2 carbon atom (see Figure 9). These transition states were about 29 kcal/mol above the reactants (F12), which is more than 10 kcal/mol higher than the transition states for

vinylhydroperoxide formation. Due to the very large excess energy of the Criegee intermediates, the 29 kcal/mol barrier alone is not sufficient to rule out the possibility of this ring-opening reaction. However, the singlet biradical peroxy-alkyl products of the reaction were only about 4 kcal/mol below the transition states in energy, and thus over 25 kcal/mol above the Criegee intermediate reactants (UωB97XD/aug-cc-pVTZ level with spin symmetry broken using the Guess=Mix keyword in Gaussian to obtain the singlet biradical wavefunction). This indicates that the reaction is highly unfavorable, and that the reverse reaction is very fast. The singlet biradical products could not be treated with a ROHF reference wavefunction, and thus F12 energy corrections could not be calculated for the singlet states of the peroxy-alkyl products. Even the F12 transition state energies for this reaction likely have large errors, as the T1 diagnostics were high; 0.043-0.048. F12 calculations on the triplet states of the product structures yielded relative energies of about 40 kcal/mol compared to the reactants. As the singlet and triplet states should be close in energy due to the large separation of the radical centres (see e.g. ref 39, where the singlet-triplet energy gap in benzyne diradicals decreases from around 36 to less than 4 kcal/mol as the radical centers are shifted from adjacent carbon atoms to carbon atoms on opposite sides of the six-membered ring), this confirms the qualitative result that the reaction is thermodynamically unfavorable. UHF-UCCSD(T)/6-31+G(d) calculations using Gaussian 09 on the ring-breaking reaction yield transition state energies about 40 kcal/mol above the reactants, and product energies about 35 kcal/mol above the reactants, suggesting that the reaction is even slower and less favorable than predicted by DFT.

This unimolecular ring-opening reaction is thus unlikely to contribute to ELVOC formation in the α-pinene + O_3 system, unless the peroxy-alkyl biradical is able to undergo very rapid and irreversible subsequent unimolecular reactions (such as ring closure by recombination of the

alkyl and peroxide radical groups). Due to the difficulty of accurately treating singlet biradicals, such reactions were not explored further in this study.

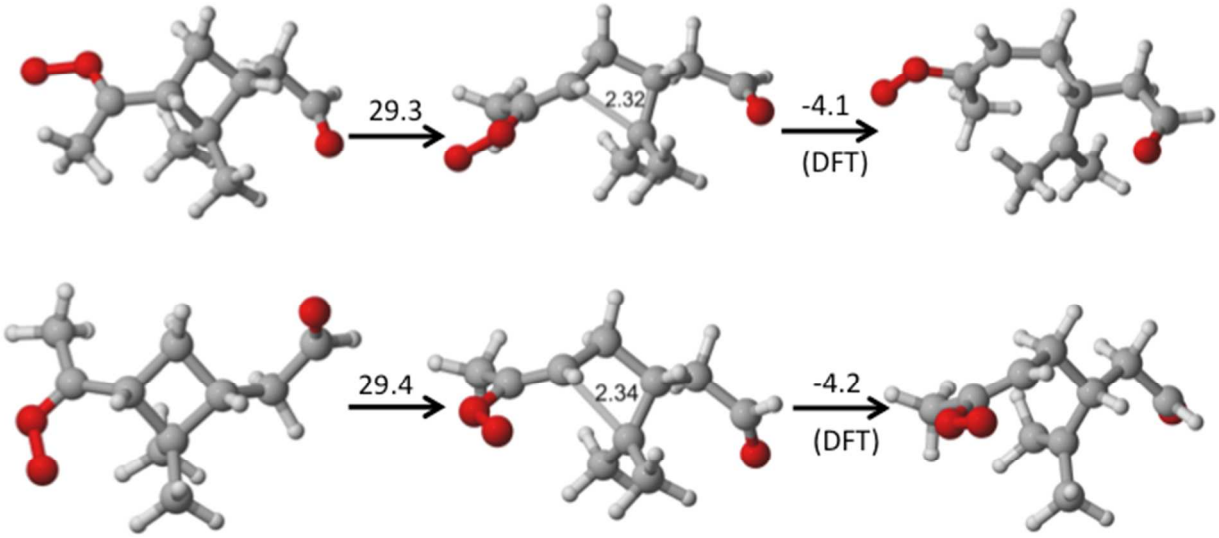

Figure 9: Reactants, transition states and products of the ring-opening channel from Criegee intermediates produced in α-pinene ozonolysis. The bond lengths of the C-C bond being broken in the transition states are given in Ångström. The reactant-to-transition state barrier has been computed at the F12 level while the transition state–to product energy difference has been computed at the UωB97XD/aug-cc-pVTZ level. Both values include zero-point corrections and are given in kcal/mol. Color coding as in Figure 3.

Ring-opening via vinoxy radicals

Fantechi et al. have investigated a ring-opening mechanism from a vinoxy radical (denoted "pinonaldehyde-d-yl-radical" by them) formed in the OH-oxidation of pinonaldehyde.[40] Exactly the same radical species is formed in α-pinene ozonolysis, via the isomerization of the terminal

syn Criegee intermediate, and subsequent OH loss from the product vinylhydroperoxide. In the vinoxy radical ring-opening reaction mechanism, the radical center is shifted to a more highly substituted carbon atom, while a new C=C bond is formed. At the B3LYP/6-31G(d,p) level, Fantechi et al. found the zero-point corrected barrier of the reaction to be 11.3 kcal/mol. This implies that the reaction is reasonably fast (with a rate constant much higher than 1 s^{-1}), but still not competitive with O_2 addition, which is generally assumed to take place in atmospheric conditions with a pseudo-unimolecular rate constant on the order of 10^7 s^{-1}. We recomputed the energetics of this reaction channel at the F12 level (see Figure 10), and found a slightly higher barrier height of 14.2 kcal/mol. Using Equation 1, we obtain a forward rate constant of 530 s^{-1} for the ring-opening (and a reverse rate constant of 1400 s^{-1}, both including an Eckart tunneling factor of 1.33). The ring-opening reaction is thus unlikely to compete with O_2 addition to the vinoxy radical, unless the latter is for some reason several orders of magnitude slower than what is normally assumed for alkyl (and vinoxy) radicals.[41]

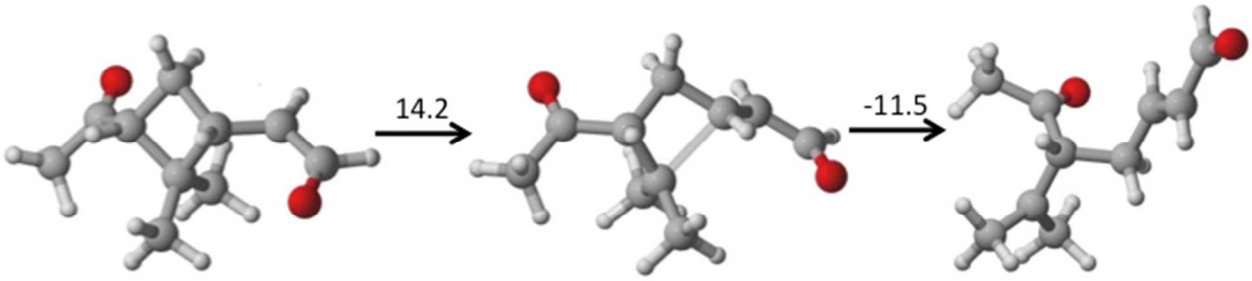

Figure 10: Reactant, transition state and product of the ring-opening channel from one of the vinoxy radicals produced in α-pinene ozonolysis. The length of the C-C bond being broken in the transition state is 2.13 Å. Zero-point corrected F12 relative energies in kcal/mol are given for each step. Color coding as in Figure 3.

Ring-opening via alkoxy radicals

Cyclic alkoxy radicals (RO), in which the radical group is located on the ring, are known to undergo prompt ring-opening reactions.[42] Peroxy radicals RO_2c and RO_2d can form such alkoxy radicals (denoted ROc and ROd) via bimolecular reactions with e.g. NO, RO_2 or HO_2. When an oxygen atom was removed from RO_2c and RO_2d, the ring promptly opened in the subsequent ωB97XD/aug-cc-pVTZ geometry optimizations. We were unable to find transition states for this ring-opening reaction. While this does not prove the complete absence of a transition state, it strongly suggests that the ring-opening of the alkoxy radicals ROc and ROd is extremely fast, and likely occurs before any other possible uni- or bimolecular reaction of the alkoxy radical. See Figure 11 for an illustration of the alkoxy – pathway for the ring-opening reaction.

The ring-opening reactions shown in Figure 11 yield an alkyl radical with three carbonyl groups, as the original alkoxy radical group has been transformed into a ketone. In Figure 12, O_2 addition to this product is illustrated schematically. This reaction would form a $C_{10}H_{15}O_5$ peroxy radical, which can likely undergo a rapid aldehydic H-shift, followed again by O_2 addition (in competition with CO loss). More speculatively, the third-generation $C_{10}H_{15}O_7$ peroxy radical might then undergo yet another H-shift, probably a 1,5 H-shift either from C5 (which now has the advantage of a tertiary carbon atom without the penalty of a strained ring), or from C7 (which is now located next to a ketone group, which enhances H-shifts[11]). Even a fourth H-shift could then be envisioned, from either C4, C5 or C7. Rapid "scrambling" of the RO_2 group by fast OOH···OO H-shifts[43] would allow for advantageous H-shift geometries (1,6 or 1,7) throughout the autoxidation chain. Ring-opening, followed by rapid H-shifts, could thus plausibly explain part the observed ELVOC products with up to 11 oxygen atoms in the α-pinene system (see

Figure 12 for a possible reaction pathway yielding a product with 9 oxygen atoms). Unfortunately, verifying the feasibility of these second- through fourth – generation H-shifts, as well as the associated uni- and bimolecular termination reactions forming the closed-shell products, is not possible at the coupled-cluster level with existing computational resources.

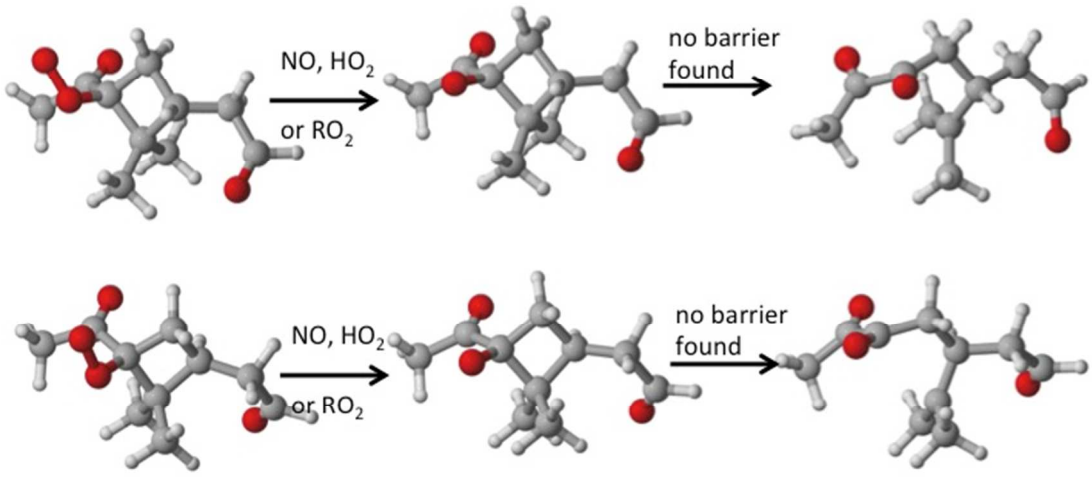

Figure 11. Schematic illustration for ring-opening reactions of peroxy radicals RO_2c and RO_2d via the alkoxy route. Color coding as in Figure 3.

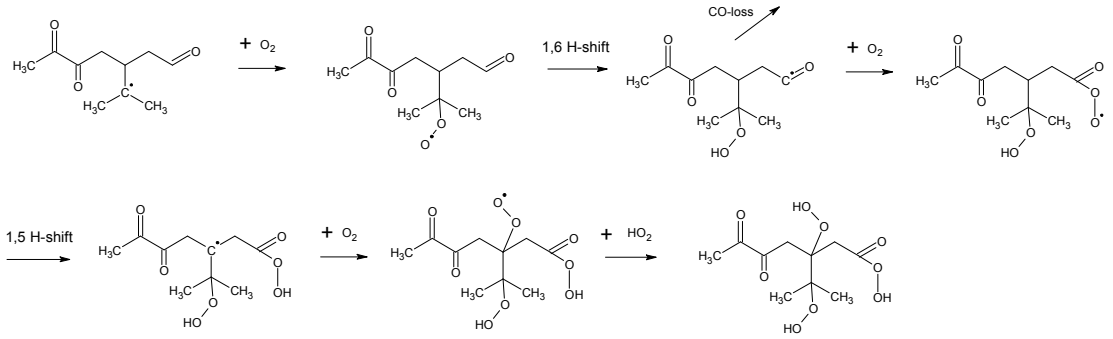

Figure 12: One possible autoxidation pathway from the products of Fig 11, yielding a $C_{10}H_{15}O_9$ peroxy radical. Reaction of this peroxy radical with HO_2 would yield a closed-shell $C_{10}H_{16}O_9$ species.

Evaluation of ring-opening mechanisms

None of the three investigated ring-opening mechanisms is able to explain all of the observed features of the α-pinene + O_3 mass spectrum (including isotope substitution effects). The Criegee intermediate – based mechanism is thermodynamically far too unfavorable, and unlikely to compete with vinylhydroperoxide formation. The vinoxy radical – based mechanism is fast, but likely unable to compete with O_2 addition, assuming that the latter occurs at similar rates as for simple alkyl radicals. The alkoxy radical – based mechanism requires a bimolecular reaction partner such as NO, HO_2 or RO_2. As described in section S3 of the Supplementary information, the HO_2 and RO_2 concentration ranges in the experiments of Ehn et al.[12] and Rissanen et al.[13,17] can be roughly estimated as 1-20×10^{10} molec. cm^{-3} and 2-50×10^{10} molec. cm^{-3}, respectively, with the NO concentration difficult to quantify but likely lower than this. If the rate constants of the alkoxy-forming RO_2 + HO_2 and RO_2 + RO_2 reactions are on the order of 10^{-12} cm^3 $molec^{-1}$ s^{-1} (with significant variation depending on the precise RO_2 reacting), then the pseudo-unimolecular rate of alkoxy radical formation could conceivably reach values around 1 s^{-1}, and the proposed ring-opening pathway could thus explain at least part of the ELVOC formation observed both in laboratory studies, and in the field. Alkoxy radical reactions have also been invoked by Mentel et al. as explanations for some of the peaks observed in the mass spectra of their chamber experiments.[14] However, the main radical species detected in the α-pinene + O_3 mass spectrum[15,17] have an even number of oxygen atoms, whereas the radicals formed from the proposed alkoxy pathway would have an odd number of oxygen atoms. Furthermore, ELVOC formation has also been observed in experiments with very low precursor concentrations (and thus RO_2 and HO_2 concentrations).[15] In these conditions, the yield of RO_2 + RO_2, RO_2 + HO_2 and RO_2 + NO reactions are expected to be negligible. Both of these findings

suggest that the alkoxy ring-opening pathway cannot explain all ELVOC observations in the α-pinene + O_3 system.

Conclusions and atmospheric implications

We have systematically investigated all possible non-methyl hydrogen shift reactions for peroxy radicals formed in the ozonolysis of α-pinene. All of these were found to be slow, with transition state theory – calculated rate constants of well below 1 s^{-1}. The formation of "ELVOC" products with O:C ratios around or above one in the α-pinene + O_3 system thus very likely requires reaction steps breaking the cyclobutyl ring left intact by the initial ozonolysis. Similar conclusions likely apply also to other alkene – oxidant combinations, where the first-generation peroxy radicals contain intact cyclopropyl or cyclobutyl rings. Both uni- and bimolecular reaction mechanism for ring-opening in atmospheric oxidation processes have been proposed in the literature, and at least three of them are in principle possible also in the α-pinene + O_3 system. Ring-opening from Criegee intermediates and vinoxy radicals is likely not competitive with alternative reaction routes (isomerization and O_2 addition, respectively). Bimolecular reactions of peroxy radicals with the RO_2 group located on the cyclobutyl ring can lead to prompt ring opening via alkoxy radical formation, but requires sufficiently high concentrations of bimolecular reaction partners. Thus, while the discussed reaction can explain some of the ELVOC formation in α-pinene + O_3 system, additional reaction mechanisms are required to explain all details of the observed α-pinene + O_3 ELVOC mass spectrum.

ACKNOWLEDGMENT

We thank the Academy of Finland, the European Research Council (grant 638703-COALA), and the Danish Council for Independent Research – Natural Sciences for funding. The CSC IT center for Science in Espoo, Finland, and the Danish Center for Scientific Computing (DCSC), are acknowledged for computer time.

Supporting Information Available. Details on the formation mechanism of the studied peroxy radicals, the MESMER calculations and the estimates of experimental RO_2 and HO_2 concentrations, as well as kinetic, energetic and structural data for all studied species. This information is available free of charge via the Internet at http://pubs.acs.org

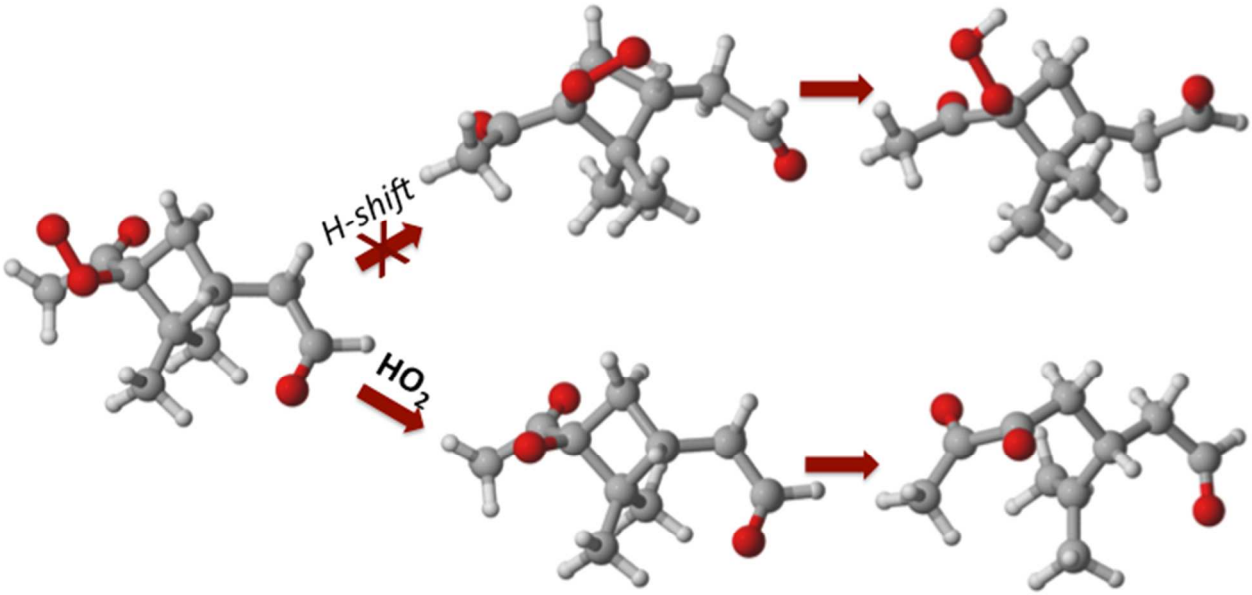

TOC Image

REFERENCES

[1] Silva, R. A.; West, J. J.; Zhang, Y.; Anenberg, S. C.; Lamarque, J.-F.; Shindell, D. T.; Collins, W. J.; Dalsoren, S.; Faluvegi, G.; Folberth, G. Global Premature Mortality Due to Anthropogenic Outdoor Air Pollution and the Contribution of Past Climate Change. *Environ. Res. Lett*. **2013**, *8*, 034005.

[2] Jimenez, J. L.; Canagaratna, M. R.; Donahue, N. M.; Prevot, A. S.; Zhang, Q.; Kroll, J. H.; DeCarlo, P. F.; Allan, J. D.; Coe, H.; Ng, N. L., et al. Evolution of Organic Aerosols in the Atmosphere. *Science* **2009**, *326*, 1525−1529.

[3] Seinfeld, J. S.; Pandis, S. N. *Atmospheric Chemistry and Physics: From Air Pollution to Climate Change, 2nd ed*. Wiley-Interscience **2006**.

[4] Glowacki, D. R.; Pilling, M. J. Unimolecular Reactions of Peroxy Radicals in Atmospheric Chemistry and Combustion. *ChemPhysChem* **2010**, *11*, 3836−3843.

[5] Orlando, J. J.; Tyndall, G. S. Laboratory Studies of Organic Peroxy Radical Chemistry: an Overview with Emphasis on Recent Issues of Atmospheric Significance. *Chem. Soc. Rev*. **2012**, *41*, 6294− 6317.

[6] Kroll, J. H.; Seinfeld, J. H. Chemistry of Secondary Organic Aerosol: Formation and Evolution of Low-volatility Organics in the Atmosphere. *Atmos. Environ*. **2008**, *42*, 3593−3624.

[7] Donahue, N. M.; Kroll, J. H.; Pandis, S. N.; Robinson, A. L. A two-dimensional volatility basis set – Part 2: Diagnostics of organic-aerosol evolution. *Atmos. Chem. Phys*. **2012**, *12*, 615–634.

[8] Pilling, M. J. Interactions Between Theory and Experiment in the Investigation of Elementary Reactions of Importance in Combustion. *Chem. Soc. Re*v. **2008**, *37*, 676−685.

[9] Peeters, J.; Müller, J.-F. HO_x Radical Regeneration in Isoprene Oxidation via Peroxy Radical Isomerisations. II: Experimental Evidence and Global Impact. *Phys. Chem. Chem. Phys.*, **2010**, *12*, 14227-14235.

[10] Vereecken, L.; Müller, J.-F.; Peeters, J. Low-Volatility Poly-Oxygenates in the OH-Initiated Atmospheric Oxidation of α-pinene: Impact of Non-Traditional Peroxyl Radical Chemistry. *Phys. Chem. Chem. Phys*. **2007**, *9*, 5241-5248.

[11] Crounse, J. D.; Nielsen, L. B.; Jørgensen, S.; Kjaergaard, H. G.; Wennberg, P. O. Autooxidation of Organic Compounds in the Atmosphere. *J. Phys. Chem. Lett.* **2013**, *4*, 3513-3520.

[12] Ehn, M.; Thornton, J. A.; Kleist, E.; Sipilä, M.; Junninen, H.; Pullinen, I.; Springer, M.; Rubach, F.; Tillmann, R.; Lee, B.; et al. A Large Source of Low-Volatility Secondary Organic Aerosol. *Nature* **2014**, *506*, 476−479.

[13] Rissanen, M. P.; Kurtén, T.; Sipilä; M.; Thornton, J. A.; Kangasluoma, J.; Sarnela, N.; Junninen, H.; Jørgensen, S.; Schallhart, S.; Kajos, M. K.; et al. The Formation of Highly Oxidized Multifunctional Products in the Ozonolysis of Cyclohexene. *J. Am. Chem. Soc*. **2014**, *136*, 15596−15606.

[14]Mentel, T. F.; Springer, M.; Ehn, M.; Kleist, E.; Pullinen, I.; Kurtén, T.; Rissanen, M.; Wahner, A.; Wildt, J. Formation of Highly Oxidized Multifunctional Compounds: Autoxidation

of Peroxy Radicals Formed in the Ozonolysis of Alkenes – Deduced from Structure–Product Relationships. *Atmos. Chem. Phys*. **2015**, *15*, 6745-6765.

[15] Jokinen, T.; Sipilä, M.; Richters, S.; Kerminen, V.-M.; Paasonen, P.; Stratmann, F.; Worsnop, D.; Kulmala, M.; Ehn, M.; Herrmann, H.; et al. Rapid Autoxidation Forms Highly Oxidized RO_2 Radicals in the Atmosphere. *Angew. Chem. Internat. Ed.* **2014**, *53*, 14596–14600.

[16] Hyttinen, N.; Kupiainen-Määttä, O.; Rissanen, M. P.; Muuronen, M.; Ehn, M.; Kurtén, T. Modeling the Charging of Highly Oxidized Cyclohexene Ozonolysis Products Using Nitrate-Based Chemical Ionization. *J. Phys. Chem. A* **2015**, *119*, 6339–6345.

[17] Rissanen, M. P.; Kurtén, T.; Sipilä, M.; Thornton, J. A.; Kausiala, O.; Garmash, O.; Kjaergaard, H. G.; Petäjä, T.; Worsnop, D. R.; Ehn, M., et al. Effects of Chemical Complexity on the Autoxidation Mechanisms of Endocyclic Alkene Ozonolysis Products: From Methylcyclohexenes toward Understanding α-Pinene. *J. Phys. Chem. A,* **2015**, *119*, 4633–4650.

[18] Spartan 14; Wavefunction Inc.: Irivine CA, **2014**.

[19] Chai, J. D.; Head-Gordon, M. Long-Range Corrected Hybrid Density Functionals with Damped Atom-Atom Dispersion Corrections. *Phys. Chem. Chem. Phys*. **2008**, *10*, 6615−6620.

[20] Frisch, M. J.; Trucks, G. W.; Schlegel, H. B.; Scuseria, G. E.; Robb, M. A.; Cheeseman, J. R.; Scalmani, G.; Barone, V.; Mennucci, B.; Petersson, G. A.; et al. Gaussian 09, Revision D.01; Gaussian, Inc.: Wallingford, CT, **2009**.

[21] Adler, T. B.; Knizia, G.; Werner, H.-J. A Simple and Efficient CCSD(T)-F12 Approximation. *J. Chem. Phys*. **2007**, *127*, 221106.

[22] Peterson, K. A.; Adler, T. B.; Werner, H. J. Systematically Convergent Basis Sets for Explicitly Correlated Wavefunctions: The Atoms H, He, B-Ne, and Al-Ar. *J. Chem. Phys*. **2008**, *128*, 084102.

[23] Werner, H.-J.; Knowles, P. J.; Manby, F. R.; Schütz, M.; Celani, P.; Knizia, G.; Korona, T.; Lindh, R.; Mitrushenkov, A.; Rauhut, G.; et al. MOLPRO, a Package of Ab Initio Programs, Version 2010.1; see http://www.molpro.net.

[24] Garden, A. L.; Paulot, F.; Crounse, J. D. ; Maxwell-Cameron, I. J.; Wennberg, P. O.; Kjaergaard, H. G. Calculation of Conformationally Weighted Dipole Moments Useful in Ion-Molecule Collision Rate Estimates. *Chem. Phys. Lett*. **2009**, *474*, 45-50.

[25] Henriksen, N. E.; Hansen, F. Y. *Theories of Molecular Reaction Dynamics: The Microscopic Foundation of Chemical Kinetics.* Oxford University Press: New York, **2008**.

[26] Eckart, C. The Penetration of a Potential Barrier by Electrons. *Phys. Rev.* **1930**, *35*, 1303-1309.

[27] Criegee, R. Mechanism of Ozonolysis. *Angew. Chem. Internat. Ed.* **1975**, *14*, 745–752.

[28] Taatjes, C. A.; Shallcross, D. E.; Percival, C. J. Research Frontiers in the Chemistry of Criegee Intermediates and Tropospheric Ozonolysis. *Phys. Chem. Chem. Phys*. **2014**, *16*, 1704-1718.

[29] Jenkin, M. E.; Saunders, S. M.; Pilling, M. J. The Tropospheric Degradation of Volatile Organic Compounds: A Protocol for Mechanism Development. *Atmos. Environ.* **1997**, *31*, 81 – 104.

[30] Saunders, S. M.; Jenkin, M. E.; Derwent, R. G.; Pilling, M. J. Protocol for the Development of the Master Chemical Mechanism, MCM v3 (Part A): Tropospheric Degradation of Non-Aromatic Volatile Organic Compounds. *Atmos. Chem. Phys*. **2003**, *3*, 161-180.

[31] Villano, S. M.; Huynh, L. K.; Carstensen, H.-H.; Dean, A. M. High-Pressure Rate Rules for Alkyl + O_2 Reactions. 1. The Dissociation, Concerted Elimination, and Isomerization Channels of the Alkyl Peroxy Radical. *J. Phys. Chem. A* **2011**, *115*, 13425–13442.

[32] Miyoshi, A. Systematic Computational Study on the Unimolecular Reactions of Alkylperoxy (RO_2), Hydroperoxyalkyl (QOOH), and Hydroperoxyalkylperoxy (O_2QOOH) Radicals. *J. Phys. Chem. A* **2011**, 115, 3301-3325.

[33] Vereecken, L.; Peeters, J. A. Structure-Activity Relationship for the Rate Coefficient of H-Migration in Substituted Alkoxy Radicals. *Phys. Chem. Chem. Phys.* **2010**, *12*, 12608−12620.

[34] Crounse, J. D.; Knap, H. C.; Ørnsø, K. B.; Jørgensen, S.; Paulot, F.; Kjaergaard, H. G.; Wennberg, P. O. On the Atmospheric Fate of Methacrolein: 1. Peroxy Radical Isomerisation Following Addition of OH and O_2. *J. Phys. Chem. A*. **2012**, *116*, 5756-5762.

[35] Vereecken, L.; Peeters, J. A. Theoretical Study of the OH- Initiated Gas-phase Oxidation Mechanism of β-Pinene ($C_{10}H_{16}$): First Generation Products. *Phys. Chem. Chem. Phys*. **2012**, *14*, 3802−3815.

[36] Vereecken, L.; Peeters, J. A. H-atom Abstraction by OH-radicals from (Biogenic) (Poly)alkenes: C−H Bond Strengths and Abstraction Rates. *Chem. Phys. Lett*. **2001**, *333*, 162−168.

[37] Glowacki, D. R.; Liang, C.-H.; Morley, Pilling, M. J. MESMER: an Open-Source Master Equation Solver for Multi-Energy Well Reactions. *J. Phys. Chem. A* **2012**, *116*, 9545-9560.

[38] Nguyen, T. L.; Peeters, J.; Vereecken, L. Theoretical Study of the Gas-Phase Ozonolysis of β-pinene. *Phys. Chem. Chem. Phys*. **2009**, *11*, 5643- 5656.

[39] Slipchenko, L. V.; Krylov, A. I. Singlet-Triplet Gaps in Diradicals by the Spin-Flip Approach: A Benchmark study. *J. Chem. Phys*. **2002**, *117*, 4694-4708.

[40] Fantechi, G.; Vereecken, L.; Peeters, J. The OH-initiated Atmospheric Oxidation of Pinonaldehyde: Detailed Theoretical Study and Mechanism Construction. *Phys. Chem. Chem. Phys*. **2002**, *4*, 5795-5805.

[41] Gutman, H.; Nelson, H. H. Gas-Phase Reactions of the Vinoxy Radical with O_2 and NO. *J. Phys. Chem*. **1983**, *87*, 3902-3905.

[42] Dibble, T. S. Reactions of the Alkoxy Radicals Formed Following OH-Addition to α-Pinene and β-Pinene. C−C Bond Scission Reactions. *J. Am. Chem. Soc*. **2001**, *123*, 4228–4234

[43] Jørgensen, S.; Knap, H. C.; Otkjær, R. V.; Jensen, A. M.; Kjeldsen, M. L. H.; Wennberg, P. O.; Kjaergaard, H. G. Ultrafast Hydrogen Shift Reactions in Hydroperoxy Substituted Organic Peroxy Radicals. *Submitted to J. Phys. Chem. A., 2015.*

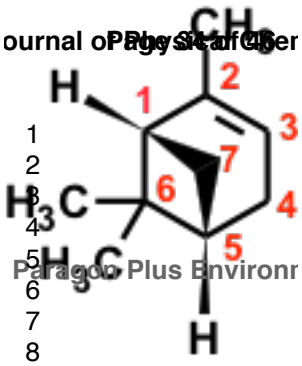

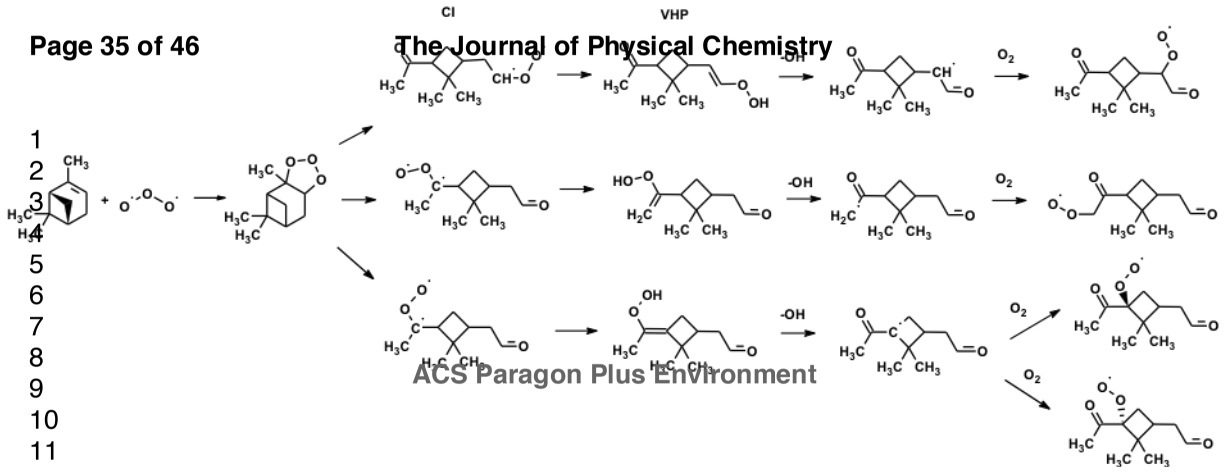

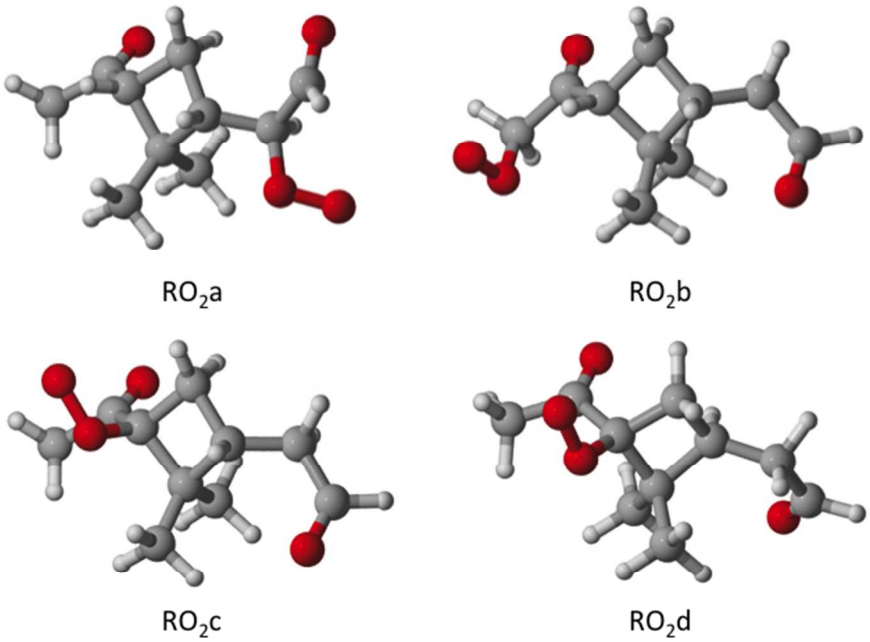

Figure 3: α-pinene ozonolysis yields four different peroxy radicals, labeled RO2a through RO2d). Color coding: gray = carbon, red = oxygen, white = hydrogen.
254x190mm (72 x 72 DPI)

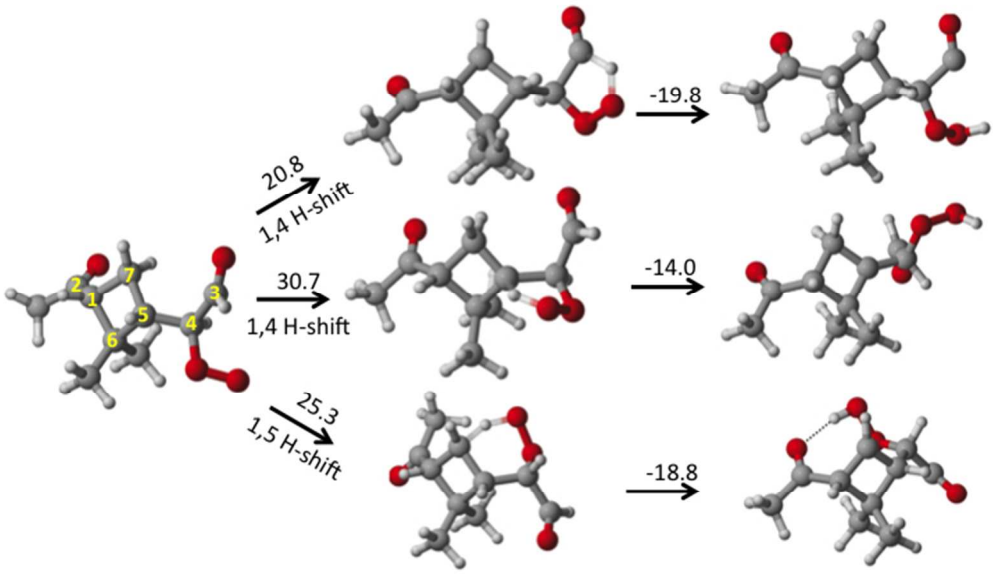

Figure 4: H-shift transition states (middle column) and products (right column) from RO2a (left). Zero-point corrected F12 relative energies in kcal/mol are given for each step. Color coding as in Figure 3. The non-methyl carbons in the reactant are numbered as in Figure 1.
254x151mm (72 x 72 DPI)

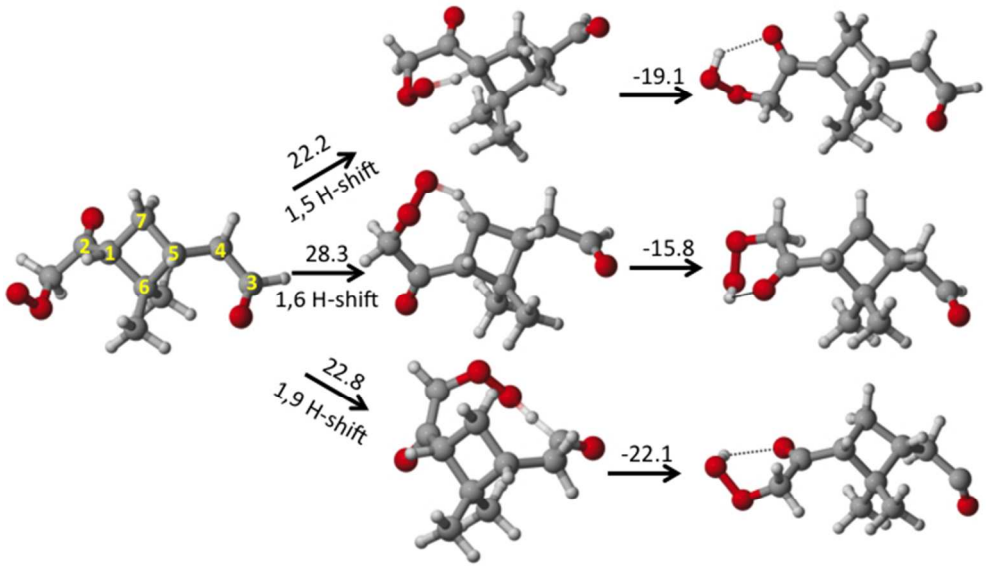

Figure 5: H-shift transition states (middle column) and products (right column) from RO2b (left). Zero-point corrected F12 relative energies in kcal/mol are given for each step. Color coding as in Figure 3. The non-methyl carbons in the reactant are numbered as in Figure 1.
254x155mm (72 x 72 DPI)

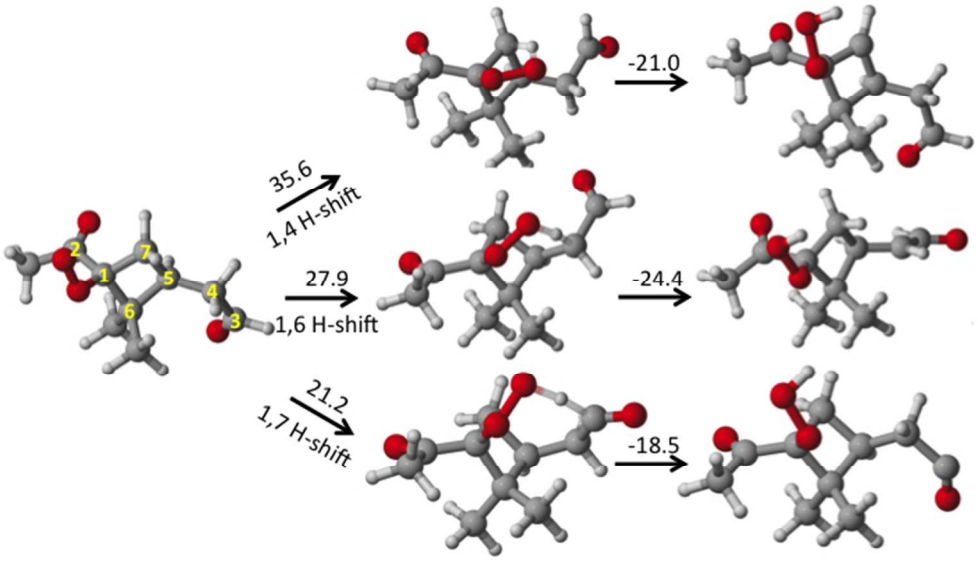

Figure 7: H-shift transition states (middle column) and products (right column) from RO2d (left). Zero-point corrected F12 relative energies in kcal/mol are given for each step. Color coding as in Figure 3. The non-methyl carbons in the reactant are numbered as in Figure 1.
254x141mm (72 x 72 DPI)

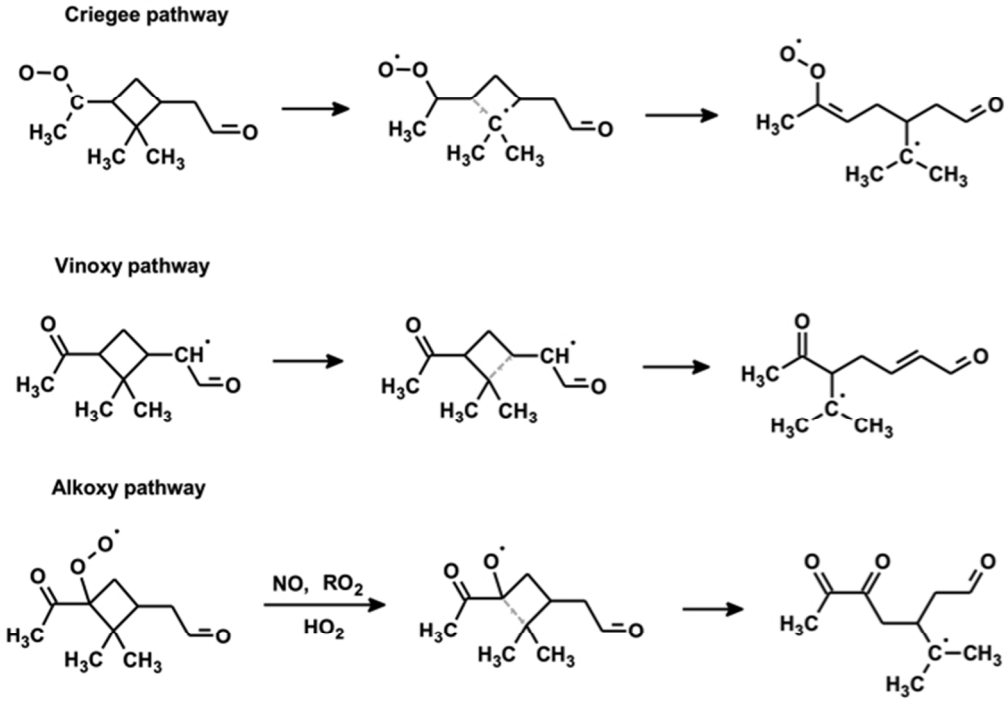

Figure 8. Three possible ring-breaking mechanisms suggested in the literature, as applied to the cyclobutyl ring in the α-pinene + O3 system.
254x190mm (72 x 72 DPI)

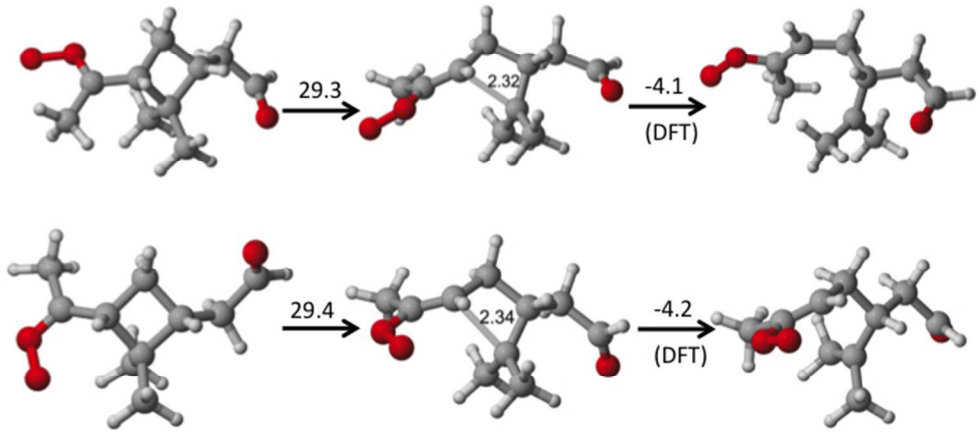

Figure 9: Reactants, transition states and products of the ring-opening channel from Criegee intermediates produced in α-pinene ozonolysis. The bond lengths of the C-C bond being broken in the transition states are given in Ångström. The reactant-to-transition state barrier has been computed at the F12 level while the transition state–to product energy difference has been computed at the UωB97XD/aug-cc-pVTZ level. Both values include zero-point corrections and are given in kcal/mol. Color coding as in Figure 3.
254x190mm (72 x 72 DPI)

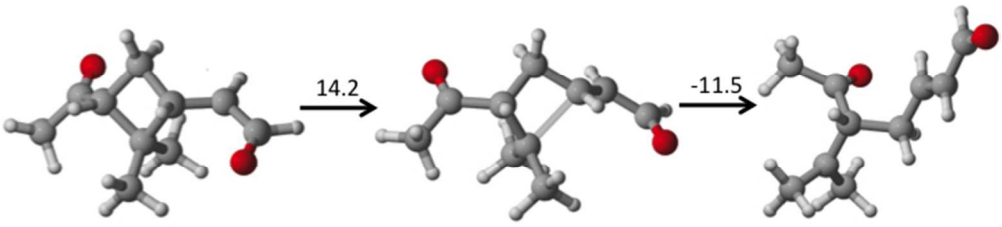

Figure 10: Reactant, transition state and product of the ring-opening channel from one of the vinoxy radicals produced in α-pinene ozonolysis. The length of the C-C bond being broken in the transition state is 2.13 Å. Zero-point corrected F12 relative energies in kcal/mol are given for each step. Color coding as in Figure 2.
254x70mm (72 x 72 DPI)

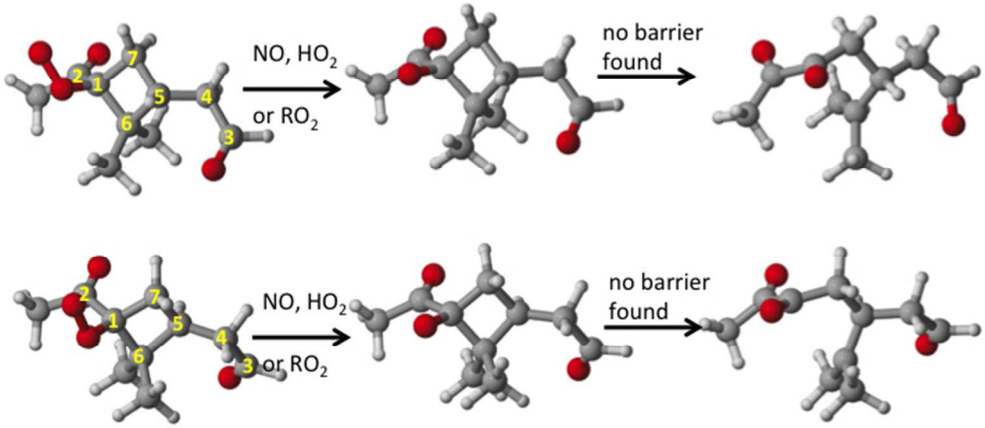

Figure 11. Schematic illustration for ring-opening reactions of peroxy radicals RO2c and RO2d via the alkoxy route. Color coding as in Figure 2. The non-methyl carbons in the reactant are numbered as in Figure 1.
254x112mm (72 x 72 DPI)

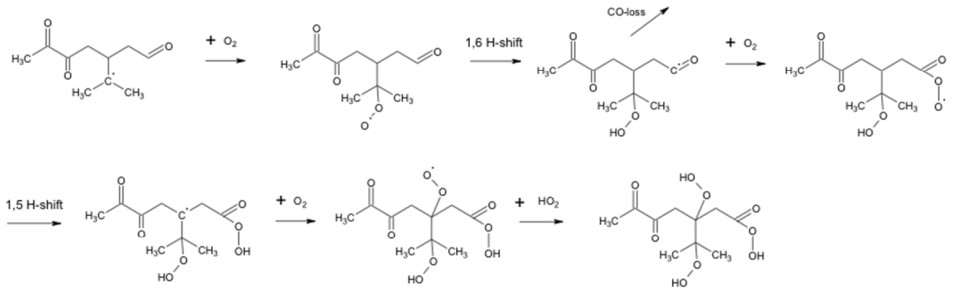

Figure 12: One possible autoxidation pathway from the products of Fig 7, yielding a C10H15O9 peroxy radical. Reaction of this peroxy radical with HO2 would yield a closed-shell C10H16O9 species.
76x25mm (300 x 300 DPI)

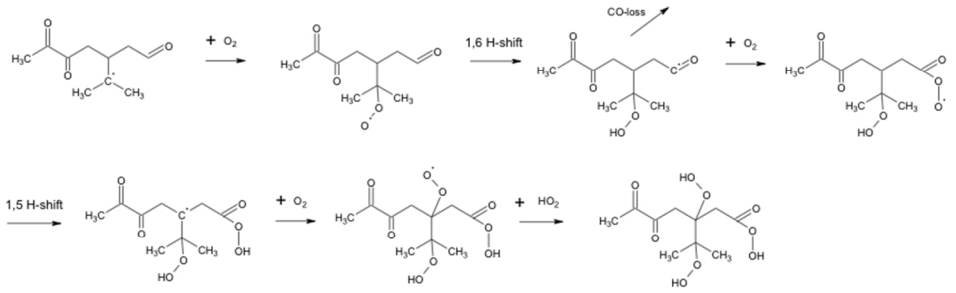

Figure 12: One possible autoxidation pathway from the products of Fig 7, yielding a C10H15O9 peroxy radical. Reaction of this peroxy radical with HO2 would yield a closed-shell C10H16O9 species.
76x25mm (300 x 300 DPI)

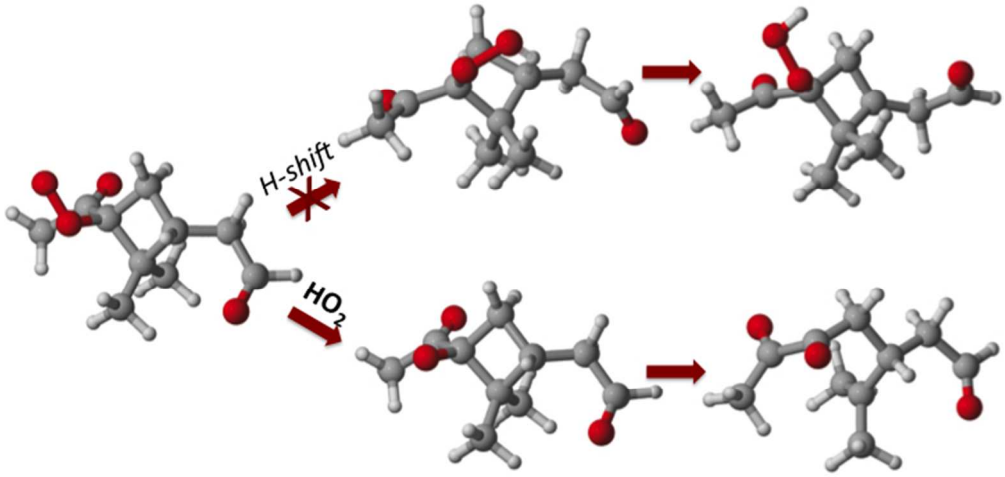

TOC image
254x127mm (72 x 72 DPI)